

chain, the polymerization degree of the arms would remain the same even after the hydrolysis. With this assumption, we calculated the block lengths of PEI and PPOZ from the integration ratio of  $C_6H_5$  (6.5–7.8 ppm) and  $NCH_2CH_2$  (2.8–3.8 ppm); this information is shown in Scheme 1.

**Keywords:** cationic polymer · micelles · porphyrinoids · self-assembly · polymers

- [1] a) P. N. Hurter, T. A. Hatton, *Langmuir* **1992**, *8*, 1291–1299; b) S. E. Webber, *J. Phys. Chem. B* **1998**, *102*, 2618–2626; c) V. Butun, A. B. Lowe, N. C. Billingham, S. P. Armes, *J. Am. Chem. Soc.* **1999**, *121*, 4288–4289; d) Y. Kakizawa, A. Harada, K. Kadaoka, *J. Am. Chem. Soc.* **1999**, *121*, 11247–11248; e) B. M. Discher, Y. Won, D. S. Ege, J. C. Lee, F. S. Bates, D. E. Discher, D. A. Hammer, *Science* **1999**, *284*, 1143–1145; f) C. Nardin, T. Hirt, J. Leukel, W. Meier, *Langmuir*, **2000**, *16*, 1035–1041; g) L. X. Chen, S. A. Jenekhe, *Macromolecules*, **2000**, *33*, 4610–4612; h) H. Shen, L. Zhang, A. Eisenberg, *J. Am. Chem. Soc.*, **1999**, *121*, 2728–2740; i) H. Shen, A. Eisenberg, *Angew. Chem.* **2000**, *112*, 3448–3450; *Angew. Chem. Int. Ed.* **2000**, *39*, 3310–3312; j) K. Schillen, K. Bryskhe, Y. Melnikova, *Macromolecules*, **1999**, *32*, 6885–6888.
- [2] a) R.-H. Jin, *Adv. Mater.* **2002**, *14*, 888–892; b) R.-H. Jin, *Macromol. Chem. Phys.* **2003**, *204*, 403–409; c) R.-H. Jin, *Chem. Commun.* **2002**, 198–199.
- [3] A. P. Nowak, V. Breedveld, L. Pakstis, B. Ozbas, D. J. Pine, D. Pochan, T. J. Deming, *Nature* **2002**, *417*, 424–428.
- [4] M. Moffitt, K. Khougaz, A. Eisenberg, *Acc. Chem. Res.* **1996**, *29*, 95–102.
- [5] a) T. Saegusa, S. Kobayashi, A. Yamada, *Macromolecules* **1975**, *8*, 390–396; b) R. Tanaka, I. Ueoka, Y. Takaki, K. Kataoka, S. Saito, *Macromolecules* **1983**, *16*, 849–853.
- [6] R.-H. Jin, K. Motoyoshi, *J. Porphyrins Phthalocyanines* **1999**, *3*, 60–64.
- [7] For example, a janus micelle with PMMA and PSt coronas was transferred into an amphiphilic janus micelle by hydrolyzing PMMA corona. See R. Erhardt, M. Zhang, A. Boker, H. Zettl, C. Abetz, P. Frederik, G. Krausch, V. Abetz, A. H. E. Muller, *J. Am. Chem. Soc.* **2003**, *125*, 3260–3267.
- [8] It was confirmed that a star poly(ethyleneimine)/HCl powder possessing a porphyrin core, which was obtained from hydrolysis of PMOZ with HCl(aq) was not soluble in 1 M HCl. In addition, it was observed that the signal due to  $(NCH_2CH_2)$  at 2.8–3.8 ppm in  $^1H$  NMR disappeared, due to formation of aggregates, when one drop of  $D_2SO_4$  was added to a  $D_2O$  solution of the polymer.
- [9] M. R. Wasielewski, *Chem. Rev.* **1992**, *92*, 435–461.
- [10] As a control experiment, a test titration was also performed for a solution of a star polymer (comprising a porphyrin center and four arms of PPOZ,  $M_w = 16400$ ,  $M_w/M_n = 1.21$ , similar to the corona backbone in the reversed micelle of **2**) in MeCN. It was found that no free-base form of the porphyrin moieties remained in the presence of 0.002 M of TA.

Received: May 6, 2003 [Z823]

## Photon Counting Histogram for One-Photon Excitation

Thomas D. Perroud, Bo Huang, Mark I. Wallace, and Richard N. Zare\*<sup>[a]</sup>

Single-molecule fluorescence is a powerful tool with which to study features hidden by an ensemble average, for example, conformational changes.<sup>[1]</sup> In many cases, optimum signal to noise is attained through the study of a few molecules at one time, which allows molecular properties to be deduced by analyzing fluctuations in the fluorescence. With this goal in mind, in 1999 Chen et al.<sup>[2]</sup> introduced the photon-counting histogram (PCH) technique to account for the fluctuations in fluorescence amplitude for molecules diffusing through a confocal laser focus. This method was first applied to two-photon fluorescence excitation. PCH was able to determine two parameters for each fluorescent species present: the average number of particles in the observation volume,  $\bar{N}$  and the molecular brightness,  $\varepsilon$ . Chen et al.<sup>[2]</sup> suggested that the same analysis procedure could be applied to one-photon excitation by using a three-dimensional Gaussian profile to describe the observation volume; however, we have found that this profile is unable to adequately fit the data. We present an alternative procedure, which is a corrected form of the 3D Gaussian profile. This procedure is able to fit the data, is easy to implement, and appears to be quite robust.

Let  $W(\vec{r})$  describe the observation volume profile, which combines the excitation strength and detection efficiency as a function of the position of a molecule. According to the PCH model, the probability of detecting  $k$  photons ( $k > 0$ ) from one fluorescent molecule in a sufficiently large reference volume  $V_0$  is<sup>[2]</sup> [Equation (1)]

$$p^{(1)}(k; V_0, \varepsilon) = \frac{1}{V_0} \int \text{Poisson}[k, \varepsilon \cdot W(\vec{r})] d\vec{r} \quad (1)$$

where  $\varepsilon$  is the molecular brightness, and [Equation (2)]

$$\text{Poisson}(k, x) = \frac{x^k e^{-x}}{k!} \quad (2)$$

is the Poisson distribution that describes the probability of getting  $k$  photons when the average number of photons received is  $x$ . Following the standard convolution procedure described by Chen et al.<sup>[2]</sup> the final form for the photon counting histogram is obtained, which is determined by two parameters for each fluorescent species: the average number of molecules in the observation volume,  $\bar{N}$ , and the molecular brightness,  $\varepsilon$ . In order to have the same  $\bar{N}$  as in fluorescence correlation spectroscopy (FCS),  $V_0$  is set proportional to the observation volume defined in FCS<sup>[3, 4]</sup> [Equation (3)]:

[a] Prof. Dr. R. N. Zare, T. D. Perroud, B. Huang, Dr. M. I. Wallace  
Department of Chemistry, Stanford University  
Stanford, California 94305-9262 (USA)  
Fax: (+1) 650-723-9262  
E-mail: zare@stanford.edu

$$V_0 = Q \cdot V_{\text{FCS}} = Q \cdot \frac{\left[ \int W(\vec{r}) d\vec{r} \right]^2}{\int W^2(\vec{r}) d\vec{r}} \quad (3)$$

where  $Q$  is chosen to be large enough so that [Equation (4)]:

$$\sum_{k=1}^{\infty} p^{(1)}(k; V_0, \epsilon) < 1 \quad (4)$$

Subsequent convolutions use a number of molecules equal to  $Q \cdot \bar{N}$  from which the value of  $\bar{N}$  can be deduced. In two-photon experiments,  $W(\vec{r})$  is well approximated by the square of the Gaussian–Gaussian–Lorentzian profile.<sup>[2]</sup> In the case of one-photon excitation experiments with confocal detection, Chen et al.<sup>[2]</sup> proposed that one should use a 3D Gaussian approximation to describe the observation volume profile, which is the same as the one used in FCS [Equation (5)]:

$$W_G(x, y, z) = \exp \left[ -\frac{2(x^2 + y^2)}{w_0^2} - \frac{2z^2}{z_0^2} \right] \quad (5)$$

where  $w_0$  is the beam waist, and  $z_0$  is the effective length of the confocal volume.

We have attempted to fit experimental one-photon excitation photon counting histograms with this 3D Gaussian PCH model for two separate samples: tetramethylrhodamine-5'-maleimide (TMR) (Figure 1 a) and Cy3-maleimide (Cy3) (Figure 1 b). We have found that at low concentration and high molecular brightness the single-species fitting fails (see Table 1). This failure is particularly distressing because these conditions are those for which PCH has the best resolution.<sup>[5]</sup> A two-species model is able to fit the data (fitting not shown); however, the fitted parameters are unphysical and contradict the FCS results on the same sample. We conclude that the 3D Gaussian model can deviate significantly from the real process, although as the molecular brightness decreases and the average number of molecules increases the deviation becomes minor (Figure 1 b).

Previous theoretical work<sup>[6, 7]</sup> has investigated the difference between the actual one-photon excitation observation volume profile  $W(\vec{r})$  and a 3D Gaussian function  $W_G(\vec{r})$ . Hess and Webb<sup>[7]</sup> point out that this deviation leads to appreciable artifacts in FCS. According to their results and our own calculations,  $W_G(\vec{r})$  well describes the observation volume profile when the molecule is close to the focal point, but  $W_G(\vec{r})$  drops much faster than  $W(\vec{r})$  when the molecule is far away from the focus. We define the signal from the difference between  $W(\vec{r})$  and  $W_G(\vec{r})$  as the out-of-focus emission profile [Equation (6)].

$$W_{\text{OOF}}(\vec{r}) = W(\vec{r}) - W_G(\vec{r}) \quad (6)$$

Although both the excitation strength and the detection efficiency are low in the out-of-focus region, its vast spatial extent makes its contribution a significant fraction of the detected photons. According to our calculations, in some conditions signal from  $W_{\text{OOF}}(\vec{r})$  can be as much as nearly half the total signal. This fact is confirmed by the calculations of Sandison and Webb<sup>[8]</sup> under paraxial approximation, in which they find the signal to background ratio (which is roughly equal

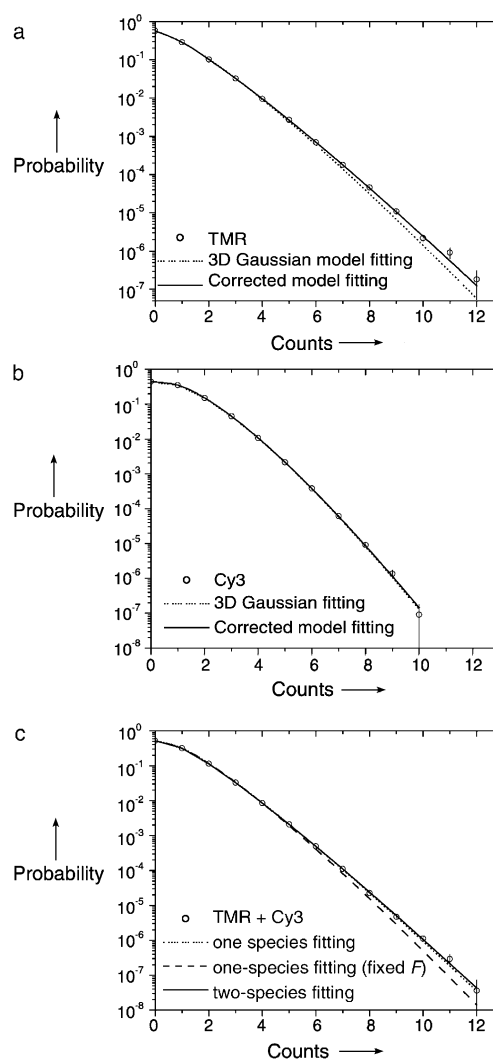


**Figure 1.** Experimental one-photon PCHs and their fittings: a) Tetramethylrhodamine-5'-maleimide (approximately 5 nm); b) Cy3-maleimide (approximately 25 nm); and c) a 1:1 mixture by volume of solutions a) and b). All measurements were made in a 20 mM HEPES buffer at pH 8.5. A higher concentration of Cy3 than TMR is used to obtain a similar overall photon count rate. Data are collected using a Nikon TE300 inverted microscope with a 60x (NA = 1.2) water immersion objective. Laser power (530 nm) is approximately 30  $\mu$ W at the sample. The  $e^{-2}$  radius of the excitation laser is approximately the same as the radius of the back aperture of the objective. The size of the confocal pinhole is 50  $\mu$ m, which gives the optimum signal-to-noise ratio in our setup. PCHs are generated with a bin time of 10  $\mu$ s. The standard deviation of the PCH is estimated using the formula proposed by Chen et al.<sup>[2]</sup> Table 1 presents the numerical results of each fit.

**Table 1.** PCH analysis with different models for data in Figure 1.

Sample	Model	$\bar{N}$	$\epsilon$	$F$	Reduced $\chi^2$
TMR	3D Gaussian	2.36	0.77	N/A	195
	corrected	2.27	1.07	0.34	0.98
Cy3	3D Gaussian	16.2	0.147	N/A	1.73
	corrected	16.1	0.213	0.44	0.75
TMR + Cy3	one species <sup>[a]</sup>	4.37	0.93	1.07	4.61
	one species (fixed F) <sup>[a]</sup>	4.51	0.60	0.38 (fixed)	259
	two species <sup>[a]</sup>	1.1	1.12	0.38	0.98
		7.0	0.21		

[a] Using the corrected model.

to the ratio of in-focus and out-of-focus emission) is 2.6 in a confocal microscope with a small pinhole. We believe this out-of-focus contribution to the total signal accounts for the failure of the 3D Gaussian PCH model to reproduce observations.

To correct for the deviation, we propose a semiempirical model that introduces one additional fitting parameter, the out-of-focus emission ratio,  $F$ , which is defined by [Equation (7)].

$$F = \frac{\int W_{\text{OOF}}(\vec{r}) d\vec{r}}{\int W_{\text{G}}(\vec{r}) d\vec{r}} \quad (7)$$

Because Equation (1) is mainly connected to the integrations of the observation volume profile, using the parameter  $F$ , we can calculate its corrected form [Equations (8a) and (8b)]:

$$p^{(1)}(k; V_0, \varepsilon) = \frac{1}{(1+F)^2} p_{\text{G}}^{(1)}(k; V_0, \varepsilon) \quad (k > 1) \quad (8a)$$

and

$$p^{(1)}(k; V_0, \varepsilon) = \frac{1}{(1+F)^2} p_{\text{G}}^{(1)}(k; V_0, \varepsilon) + \frac{F}{(1+F)^2} \cdot \frac{1}{2\sqrt{2}} \cdot \varepsilon \quad (k = 1) \quad (8b)$$

where  $p_{\text{G}}^{(1)}(k; V_0, \varepsilon)$  is the integration using the 3D Gaussian approximation. Note that our model is based on two approximations: 1) The absolute value of  $W_{\text{OOF}}(\vec{r})$  is small, so that when  $n > 1$ , the integration of the  $n$ th power of  $W_{\text{OOF}}(\vec{r})$  is negligible compared with that of  $W_{\text{G}}(\vec{r})$ ; 2)  $W_{\text{G}}(\vec{r})$  well fits the observation volume profile when close to the focus; therefore,  $W_{\text{G}}(\vec{r})$  and  $W_{\text{OOF}}(\vec{r})$  do not overlap. Details of the derivation will be presented in a future publication.

We find that this corrected model is able to fit the two experimental photon counting histograms shown in Figures 1a and 1b, as shown in Table 1. To test the validity and robustness of the corrected model, we varied the dye concentration by a factor of 20 and the laser power by a factor of 6. As Table 2 shows, as

**Table 2.** PCH analysis of TMR at different concentrations. The first row corresponds to a concentration of about 1 nM.  $\langle k \rangle$  is the average fluorescence photon count rate.  $\bar{N}_{\text{FCS}}$  is the average number of molecules in the confocal volume determined by FCS. The bin time of PCH is 20  $\mu\text{s}$ .

Relative Concentration	$\langle k \rangle$ [kHz]	$\bar{N}_{\text{FCS}}$	$\bar{N}_{\text{PCH}}$	$\varepsilon$	$F$	$\bar{N}_{\text{PCH}}/0.50$
1	15.9	0.40	0.50	2.62	0.45	1.0
5	79.7	1.94	2.33	2.65	0.39	4.7
10	161.1	4.05	4.79	2.59	0.36	9.6
20	326.6	8.41	10.81	2.30	0.35	21.6

the concentration is varied, the value of  $\varepsilon$  is nearly constant whereas the value of  $\bar{N}$  scales with the concentration. Table 3 shows that  $\bar{N}$  is essentially constant whereas the value of  $\varepsilon$  scales with the laser intensity. In all these measurements, which were taken with the same optical setup, we find that the concentration, laser intensity, and type of fluorophore hardly affect the value of  $F$ .

**Table 3.** PCH analysis of TMR (about 5 nM) at different laser powers. The first row corresponds to a laser intensity of approximately 15  $\mu\text{W}$  at the sample.  $\langle k \rangle$  is the average fluorescence photon count rate. The bin time of PCH is 20  $\mu\text{s}$ .

Relative Power	$\langle k \rangle$ [kHz]	$\bar{N}_{\text{PCH}}$	$\varepsilon$	$F$	$\varepsilon/1.26$
1.0	36.7	2.40	1.26	0.43	1.0
1.8	65.3	2.36	2.20	0.43	1.7
4.2	146.1	2.50	4.76	0.43	3.8
6.3	216.1	2.57	6.76	0.42	5.4

To confirm that this corrected PCH model is able to resolve fluorescent species with different degrees of brightness, we mixed equal amounts of the two samples in Figures 1a and 1b and measured its resulting PCH. The one-species PCH model can fit the PCH only when  $F$  goes to an unreasonable value greater than 1, whereas the two-species fitting gives the expected results: molecular brightness unchanged and the number of particles halved upon mixing (see Table 1).

In conclusion, we have presented a means of carrying out the photon-counting histogram procedure of Chen et al.<sup>[2]</sup> for one-photon excitation. Because one-photon excitation is so common in single-molecule studies, the method we have presented should be of wide applicability.

## Acknowledgements

T.D.P. thanks the Roche Research Foundation for a graduate fellowship and B.H. is grateful for a Stanford Graduate Fellowship. This work was supported by the National Institute of Health (Grant no.: 5 RO1 NS28471).

**Keywords:** fluorescence • fluorescence spectroscopy • one-photon excitation • photon counting histogram • single-molecule studies

- [1] A. A. Deniz, T. A. Laurence, M. Dahan, D. S. Chemla, P. G. Schultz, S. Weiss, *Annu. Rev. Phys. Chem.* **2001**, *52*, 233–253.
- [2] Y. Chen, J. Muller, P. So, E. Gratton, *Biophys. J.* **1999**, *77*, 553–567.
- [3] N. L. Tompson, in *Fluorescence correlation spectroscopy, Vol. 1* (Ed.: J. R. Lakowicz), Plenum Press, New York, **1991**, 337–378.
- [4] T. Wohland, R. Rigler, H. Vogel, *Biophys. J.* **2001**, *80*, 2987–2999.
- [5] J. Muller, Y. Chen, E. Gratton, *Biophys. J.* **2000**, *78*, 474–486.
- [6] H. Qian, E. L. Elson, *Appl. Opt.* **1991**, *30*, 1185–1195.
- [7] S. Hess, W. Webb, *Biophys. J.* **2002**, *83*, 2300–2317.
- [8] D. R. Sandison, W. W. Webb, *Appl. Opt.* **1994**, *33*, 603–615.

Received: May 6, 2003 [Z824]